Unified scheme for describing time delay and time advance in the interpolation of rotational bands of resonances

Enrico De Micheli*
IBF—Consiglio Nazionale delle Ricerche, Via De Marini, 6-16149 Genova, Italy

Giovanni Alberto Viano†
Dipartimento di Fisica, Università di Genova, Istituto Nazionale di Fisica Nucleare, sezione di Genova, Via Dodecaneso, 33-16146 Genova, Italy

(Received 12 September 2003; published 16 December 2003)

In this paper we show how rotational bands of resonances can be described by using trajectories of poles of the scattering amplitude in the complex angular momentum plane: each band of resonances is represented by the evolution of a single pole lying in the first quadrant of the plane. The main result of the paper consists in showing that also the antiresonances (or echoes) can be described by trajectories of the scattering amplitude poles, instead of using the hard-sphere potential scattering as prescribed by the classical Breit-Wigner theory. The antiresonance poles lie in the fourth quadrant of the complex angular momentum plane, and are associated with nonlocal potentials which take into account the exchange forces; it derives a clear-cut separation between resonance and antiresonance poles. The evolution of these latter poles describes the passage from quantum to semiclassical physics. The theory is tested on the rotational band produced by α-α elastic scattering and on the hadronic rotational bands in π^+-p elastic scattering.

DOI: 10.1103/PhysRevC.68.064606 PACS number(s): 25.70.Bc, 25.70.Ef

I. INTRODUCTION

The standard partial-wave expansion of the scattering amplitude can be regarded as a factorization which splits the scattering amplitude into two factors: the partial-wave amplitudes $a_\ell(E)$ (E being the center of mass energy, ℓ the angular momentum) and the Legendre polynomials. Therefore it permits to separate those features of the physical process that depend on the geometry or symmetry properties of the system, here represented by the Legendre polynomials, from those depending on the forces acting between the interacting particles, here described by the partial-wave amplitudes. We are thus led to a separation between dynamics and symmetry. Accordingly, the classical nuclear theory describes the cross-section peak due to a resonance by fixed poles of the scattering amplitude in the complex momentum plane, which arise in complex conjugate pairs corresponding to k and $-k^*$ ($k^2=E$ in suitable units), while the angular distribution is described by the Legendre polynomials. The theory does not attempt to group resonances in families, and provides only a local description in the neighborhood of the energy position of the resonance. On the other hand, the phenomenology shows clearly that the resonances appear in ordered sequences, such as rotational bands, which reflect the dynamical symmetries.

From the factorization between dynamics and symmetry it also follows that the angular distribution of the resonances, described by the Legendre polynomials (which are related to the unitary irreducible representation of the rotation group), cannot be in any way connected to the lifetime of the resonances. On the contrary, when the colliding particles are not identical, and therefore the scattering amplitude is not symmetrized (or antisymmetrized), the angular distribution retains memory of the incident beam direction and, consequently, it presents an asymmetry which is inversely related to the lifetime.

Another peculiar feature of the classical theory is that while the resonances are described by singularities of the scattering amplitude (Breit-Wigner poles), the antiresonances are described by the so-called potential scattering, whose amplitude is the same as the one for the scattering by an impenetrable sphere: hard-core scattering. Resonances and antiresonances are depicted with completely different models. Furthermore, the exchange forces, which play a fundamental role in producing antiresonances, are not faithfully represented by the hard-core model. It follows that in the Breit-Wigner formalism the time delay due to the resonance cannot be neatly separated from the time advance due to the antiresonance.

Finally, the classical theory, which makes use of fixed poles, does not describe the dynamical evolution of resonances and antiresonances. Instead, the phenomenology shows that the resonance widths increase with energy, and the antiresonances tend to disappear at those energies where there is a smooth transition from quantum to semiclassical behavior.

In this paper we try to recover the global character of the sequences of resonances, and specifically of the rotational bands. With this in mind, we shall represent the cross-section peaks due to resonances by the use of singularities of the scattering amplitude in the complex plane of the angular momentum, which is the generator of the rotation group. This can be achieved through a Watson-type resummation of the partial-wave expansion. Furthermore, we aim to describe

*FAX: +39 0106475500. Email address: demicheli@ge.cnr.it
†FAX: +39 010314218. Email address: viano@ge.infn.it.

resonances and antiresonances with analogous mathematical structures: i.e., scattering amplitude singularities in the complex angular momentum plane.

In a previous paper [1]—hereafter referred to as I—we studied ion collisions treating the composed structure of the clusters by means of the Jacobi coordinates and of the related SU(n)-group algebra. We proved that rotational bands emerge by removing the SU(n) degeneracies by introducing forces that depend on the relative angular momentum of the clusters: i.e., nonlocal potentials. The latter is indeed generated by the exchange forces which enter the game precisely in connection with antiresonances. In the present paper we start from the results obtained in I; next we proceed to a Watson-type resummation of the partial-wave expansion. This procedure requires some additional constraints which limit the class of nonlocal potentials admitted. We can thus study the singularities of the scattering amplitude in the complex angular momentum plane. We find that there exist two types of pole—singularities with $\mathrm{Im}\,\lambda \neq 0$ (λ denoting the complex angular momentum): the poles lying in the first quadrant (i.e., $\mathrm{Im}\,\lambda > 0$), which describe the resonances; the poles lying in the fourth quadrant (i.e., $\mathrm{Im}\,\lambda < 0$), which correspond to antiresonances. These last poles are a peculiar property of nonlocal potentials. Another characteristic feature of the complex angular momentum poles is that their location varies as a function of the energy; they are *moving poles* and, accordingly, we can speak of *pole trajectories*. The main results which we prove in this paper are the following.

(i) Each rotational band of resonances is described by the trajectory of a single pole located in the first quadrant of the complex angular momentum plane (i.e., $\mathrm{Im}\,\lambda > 0$).

(ii) The corresponding antiresonances are described by the trajectory of a single pole located in the fourth quadrant of the complex angular momentum plane (i.e., $\mathrm{Im}\,\lambda < 0$).

(iii) The pure resonance widths Γ_R can be determined from the locations of poles in the first quadrant (resonance poles) and from their dependence on the energy.

(iv) Both resonances and antiresonances are represented by pole singularities of the scattering amplitude: we thus obtain a unified scheme for describing time delay and time advance associated with the two processes.

(v) We can describe the evolution of the rotational resonances into surface waves.

These results represent a very relevant improvement with respect to our previous analysis (see Refs. [2–4]). In fact, in these latter works the rotational resonances were fitted by using trajectories of the scattering amplitude poles lying in the first quadrant of the complex angular momentum plane, whereas the antiresonances were described by the hard-sphere potential scattering in a form very similar to the classical Breit-Wigner theory.

At this point we must strongly remark that Γ_R cannot be identified with the width Γ of the peak of the observed (experimental) cross section. Indeed, the effect of the antiresonance distorts the bell-shaped structure of the pure resonance peak and, while we have a theoretical evaluation of Γ_R, we can only find an estimate of Γ through statistical procedures, as it will be discussed in Sec. V.

In the complex angular momentum representation of the physical spectrum the bound states are described by pole singularities lying on the real positive semiaxis of the λ plane (i.e., $\mathrm{Re}\,\lambda \geqslant 0, \mathrm{Im}\,\lambda = 0$). Moving from bound states to resonances, the poles enter the first quadrant, $\mathrm{Im}\,\lambda$ increases with the energy and describes the increase of the resonance widths Γ_R. At higher energy inelastic and reaction channels open, and the scattering target appears as a ball partially or totally opaque at the center: the resonances evolve into diffractive surface waves. This evolution is still described by the increase of $\mathrm{Im}\,\lambda$ with energy. Similarly, the singularities in the fourth quadrant move away from the real axis, and at high energy their contribution becomes irrelevant. This behavior concords with the fact that the antiresonances, which are produced by exchange forces, are a quantum effect which disappears at the classical level.

The paper is organized as follows. In Sec. II we outline the scattering theory for nonlocal potentials, summarizing the results obtained previously in I. In Sec. III the singularities of the scattering amplitude in the complex angular momentum plane are studied; the formulas that represent the phase shifts, and which allow us to interpolate the rotational resonances, are given. In Sec. IV we analyze the main properties of these singularities and their behavior for high values of the energy; the transition from quantum-mechanical effects to classical behavior is discussed and, accordingly, the evolution of rotational resonances in surface waves is described in detail. In Sec. V we present a phenomenological analysis in order to check the theory. In this section we reconsider the previous phenomenological work on the α-α elastic collision [3], and on the resonances and surface waves present in the π^+-p elastic scattering [4].

II. OUTLINE OF THE SCATTERING THEORY FOR NONLOCAL POTENTIALS

In this section we sketch the main results obtained in I, which are essential to perform a Watson-type resummation of the partial-wave expansion, and which enable the analysis of the scattering amplitude singularities in the complex angular momentum plane.

In I we derived and studied the following integro-differential equation of Schrödinger type:

$$(-\Delta + V_D)\chi(\mathbf{R}) + g\int_{\mathbb{R}^3} V(\mathbf{R},\mathbf{R}')\chi(\mathbf{R}')d\mathbf{R}' = E\chi(\mathbf{R}), \tag{1}$$

which describes the interaction of two clusters. In Eq. (1) Δ is the relative-motion kinetic energy operator, g is a real coupling constant, V_D is the potential which derives from direct forces, $V(\mathbf{R},\mathbf{R}')$ represents the nonlocal potential which takes into account the exchange forces and, finally, E represents, in the case of the scattering process, the relative kinetic energy of the two clusters in the center of mass system ($\hbar = 2\mu = 1$, μ being the reduced mass of the clusters). From the current conservation law it follows that

$V(\mathbf{R},\mathbf{R}')$ is a real and symmetric function: $V(\mathbf{R},\mathbf{R}')=V^*(\mathbf{R},\mathbf{R}')=V(\mathbf{R}',\mathbf{R})$; moreover, $V(\mathbf{R},\mathbf{R}')$ depends only on the lengths of the vectors $\mathbf{R},\mathbf{R}'$ and on the angle γ between them, or equivalently, on the dimension of the triangle with vertices $(0,\mathbf{R},\mathbf{R}')$ but not on its orientation. Hence, $V(\mathbf{R},\mathbf{R}')$ can be formally expanded as follows:

$$V(\mathbf{R},\mathbf{R}')=\frac{1}{4\pi RR'}\sum_{s=0}^{\infty}(2s+1)V_s(R,R')P_s(\cos\ \gamma), \quad (2)$$

where $\cos\gamma=(\mathbf{R}\cdot\mathbf{R}')/(RR')$, $R=|\mathbf{R}|$, and P_s are the Legendre polynomials. The Fourier-Legendre coefficients $V_s(R,R')$ are given by

$$V_s(R,R')=4\pi RR'\int_{-1}^{1}V(R,R';\cos\ \gamma)P_s(\cos\ \gamma)d(\cos\ \gamma). \quad (3)$$

We may therefore state that the left hand side operator of Eq. (1), acting on the wave function χ, is a formally Hermitian and rotationally invariant operator.

Next, we expand the relative-motion wave function $\chi(\mathbf{R})$ in the form

$$\chi(\mathbf{R})=\frac{1}{R}\sum_{\ell=0}^{\infty}\chi_\ell(R)P_\ell(\cos\ \theta), \quad (4)$$

where now ℓ is the relative angular momentum between the clusters.

Since γ is the angle between the two vectors $\mathbf{R}$ and $\mathbf{R}'$, whose directions are determined by the angles (θ,ϕ) and (θ',ϕ'), respectively, we have $\cos\gamma=\cos\theta\cos\theta'+\sin\theta\sin\theta'\cos(\phi-\phi')$. Then, by using the following addition formula for the Legendre polynomials:

$$\int_0^{\pi}\int_0^{2\pi}P_s(\cos\ \gamma)P_\ell(\cos\ \theta')\sin\ \theta'd\theta'd\phi'=\frac{4\pi}{(2\ell+1)}P_\ell(\cos\ \theta)\delta_{s\ell}, \quad (5)$$

from Eqs. (1), (2), (4), and (5) we obtain

$$\chi_\ell''(R)+k^2\chi_\ell(R)-\frac{\ell(\ell+1)}{R^2}\chi_\ell(R)=g\int_0^{+\infty}V_\ell(R,R')\chi_\ell(R')dR', \quad (6)$$

where $k^2=E$, and the local potential is now supposed to be included in the nonlocal one.

As in I, we suppose that $V(\mathbf{R},\mathbf{R}')$ is a measurable function in $\mathbb{R}^3\times\mathbb{R}^3$, and that there exists a constant α such that

$$C=\left\{\int_{\mathbb{R}^3}(1+R^2)e^{2\alpha R}d\mathbf{R}\int_{\mathbb{R}^3}(1+R'^2)R'^2e^{2\alpha R'}\times|V(\mathbf{R},\mathbf{R}')|^2d\mathbf{R}'\right\}^{1/2}<\infty. \quad (7)$$

If bound (7) is satisfied, then expansion (2) converges in the norm $L^2(-1,1)$ for almost every $R,\ R'\in[0,+\infty)$.

We must distinguish between two kinds of solutions to Eq. (6): the scattering solutions $\chi_\ell^{(s)}(k,R)$, and the bound-state solutions $\chi_\ell^{(b)}(R)$:

(i) The scattering solutions satisfy the following conditions:

$$\chi_\ell^{(s)}(k,R)=kRj_\ell(kR)+\Phi_\ell(k,R), \quad (8a)$$

$$\Phi_\ell(k,0)=0;\ \lim_{R\to+\infty}\left\{\frac{d}{dR}\Phi_\ell(k,R)-ik\Phi_\ell(k,R)\right\}=0, \quad (8b)$$

where $j_\ell(kR)$ are the spherical Bessel functions, and the functions $d\Phi_\ell/dR$ are supposed to be absolutely continuous.

(ii) The bound-state solutions $\chi_\ell^{(b)}(R)$ satisfy the conditions

$$\int_0^{+\infty}|\chi_\ell^{(b)}(R)|^2dR<\infty,\ \ \chi_\ell^{(b)}(0)=0. \quad (9)$$

Then, one can compare, as in the case of local potentials, the asymptotic behavior of the scattering solution, for large values of R, with the asymptotic behavior of the free radial function $j_\ell(kR)$, and correspondingly, introduce the phase shifts $\delta_\ell(k)$; accordingly, we can define the scattering amplitude

$$T_\ell(k)=e^{i\delta_\ell(k)}\sin\ \delta_\ell(k). \quad (10)$$

Now, we can introduce, as in the standard collision theory, the total scattering amplitude that, in view of the rotational invariance of the total Hamiltonian, can be formally expanded in terms of Legendre polynomials as follows:

$$f(E,\theta)=\sum_{\ell=0}^{\infty}(2\ell+1)a_\ell(E)P_\ell(\cos\ \theta), \quad (11)$$

where E is the center of mass energy, θ is the center of mass scattering angle, ℓ is the relative angular momentum of the colliding clusters, and the partial scattering amplitudes $a_\ell(E)$ are given by

$$a_\ell(E)=\frac{e^{2i\delta_\ell}-1}{2ik}=\frac{T_\ell(k)}{k}\ \ (k^2=E;2\mu=\hbar=1). \quad (12)$$

Expansion (11) factorizes the amplitude into kinematics and dynamics: the Legendre polynomials $P_\ell(\cos\theta)$ (which are related to the unitary irreducible representation of the rotation group) describe the kinematics: the coefficients $a_\ell(E)$ (and specifically their singularities) reflect the dynamics. On this factorization is indeed based the classical Breit-Wigner theory of resonances, which separates kinematics from dynamics. But, as already mentioned, in this way the global aspect of the families of states, such as the rotational bands, is lost. To recover the global aspect of the rotational bands, as suggested by the phenomenological data, one could try to represent the dynamics through the singularities (poles) in the complex plane of the angular momentum, which is the generator of the rotation

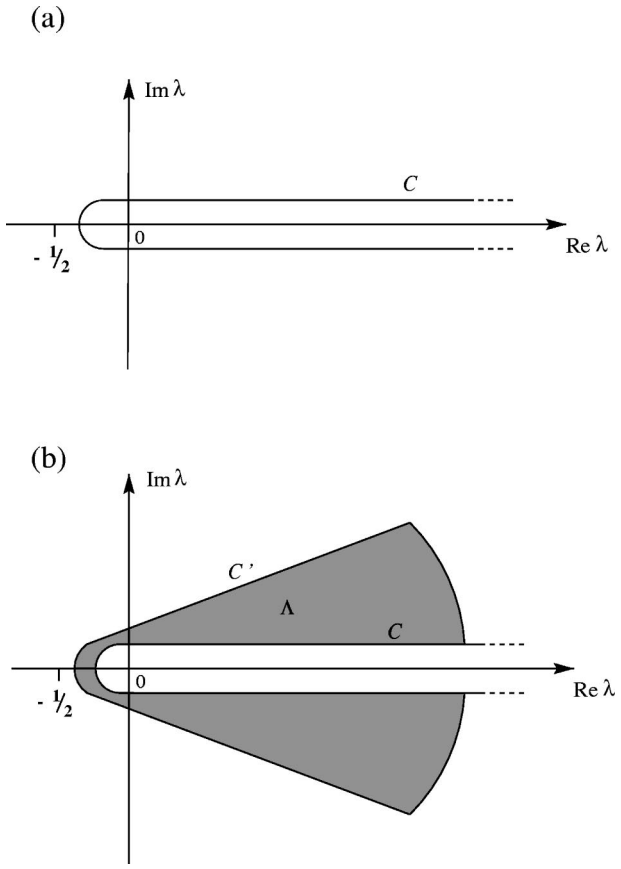

FIG. 1. (a) Integration path of integral in formula (13). (b) Integration path of integral in formula (15).

group. This can be achieved through a Watson resummation of expansion (11), which consists in regarding the partial-wave series as an infinite sum over the residues of the poles of the function $1/\sin \pi\lambda$, obtained by the following integral whose integration path C is shown in Fig. 1(a):

$$f(E,\theta)=\frac{i}{2}\int_C \frac{(2\lambda+1)a(\lambda,E)P_\lambda(-\cos\theta)}{\sin\pi\lambda}d\lambda. \quad (13)$$

In order to deform conveniently the path C, it is usually assumed that the partial waves $a_\ell(E)$ are the restriction to the integers of a function $a(\lambda,E)$ ($\lambda\in\mathbb{C}, E$ fixed) meromorphic in the half plane $\mathrm{Re}\,\lambda>-1/2$, holomorphic for $\mathrm{Re}\,\lambda>L-1/2$ (where L is an integer larger than zero). All these properties are satisfied by the partial waves associated with the class of the Yukawian potentials [5]. In the case of nonlocal potentials some peculiar features emerge because not only the centrifugal barrier, but also the potential itself depends on the angular momentum. Therefore, some results concerning the restriction on the position of the poles of the S function $S(\lambda,k)=\exp[2i\delta(\lambda,k)]$ ($\lambda\in\mathbb{C}$, $\mathrm{Re}\,\lambda>-1/2$, k real and fixed) fail in this case. We can note, as a typical example of this situation, that while for the class of the Yukawian potentials no poles of the S function occur for $\mathrm{Im}\,\lambda<0$, this is not the case for potentials which depend on the angular momentum.

By adding suitable constraints to the conditions introduced previously, one can prove that in the complex angular momentum plane there exists an angular sector Λ where the partial amplitudes $a(\lambda,k)$ satisfy the following bound [6]:

$$a(\lambda,k)=O(e^{-\beta\lambda})\big(\lambda\in\Lambda,\mathrm{Re}\,\lambda\to+\infty;\beta>0\big). \quad (14)$$

Accordingly, the contour C can be deformed into the contour C', as shown in Fig. 1(b). We thus obtain

$$f(E,\theta)=\frac{i}{2}\int_{C'}\frac{(2\lambda+1)a(\lambda,E)P_\lambda(-\cos\theta)}{\sin\pi\lambda}d\lambda + \sum_{n=1}^{N}\frac{g_n(E)P_{\lambda_n}(-\cos\theta)}{\sin\pi\lambda_n(E)}, \quad (15)$$

where $\lambda_n(E)=\alpha_n(E)+i\beta_n(E)$ give the location of the amplitude poles belonging to the angular sector Λ of the λ plane [see Fig. 1(b)], and lying either in the first or in the fourth quadrant; $g_n(E)$ are the residues of $(2\ell+1)a_\ell(E)$ at the poles. It is worth remarking that in the applications to low-energy nuclear physics, which are our concern, the path C' not necessarily has to run parallel to the imaginary axis, as in the case of the high-energy physics. In fact, we are working in the physical region of $\cos\theta(-1\leqslant\cos\theta\leqslant1)$, and we are not interested in the asymptotic behavior of the scattering amplitude for large transmitted momentum.

III. COMPLEX ANGULAR MOMENTUM REPRESENTATION OF RESONANCES AND ANTIRESONANCES

First let us consider the poles lying in the first quadrant and within the angular sector Λ [see Fig. 1(b)]; suppose that at a certain energy, and for a specific value n_0 of n, α_{n_0} crosses an integer, while $\beta_{n_0}\ll1$; then the corresponding term in the sum over the poles in representation (15) becomes very large: we have a pole dominance. Therefore, in the neighborhood of a sharp and isolated resonance the following approximation for the amplitude is worth trying:

$$f(E,\theta)\simeq g(E)\frac{P_\lambda(-\cos\theta)}{\sin\pi\lambda(E)} \quad (16)$$

(for simplicity, we have dropped the subscript n_0). The Legendre function $P_\lambda(-\cos\theta)$ presents a logarithmic singularity at $\theta=0$ [7,8]. Therefore, approximation (16) certainly breaks down forwards, where it is necessary to take into account also the contribution of the background integral, in order to make the amplitude $f(E,\theta)$ finite and regular. Conversely, approximation (16) is satisfactory at backward angles. The logarithmic singularity, which the Legendre functions $P_\lambda(-\cos\theta)(\lambda\in\mathbb{C})$ present at $\theta=0$, clearly indicates that the angular distribution given by these functions, and, accordingly, by approximation (16), is asymmetric. However, let us observe that this peculiar feature of approximation (16) should not be regarded as a defect, but it could be interpreted as the capability of this representation of displaying the specific aspect of the resonances of nonidentical particles, i.e., the asymmetry

proper of the unstable states. Since the angular lifetime is finite, the isotropy in θ is broken: there is memory of the incident beam direction. The angular asymmetry proper of the resonances can then be associated with the *spin width* of the compound state (see I, Sec. 4): to small values of angular momentum dispersion there corresponds a small degree of asymmetry in the angular distribution.

Amplitude (16) diverges logarithmically forward and the differential cross section diverges as the square of the logarithm, but the total cross section, derived from Eq. (16), is finite. Indeed, we have

$$\sigma_{\text{tot.}} = \frac{2\pi|g(E)|^2}{|\sin\ \pi\lambda(E)|^2}\int_0^\pi |P_\lambda(-\cos\ \theta)|^2 \sin\ \theta d\theta, \qquad (17)$$

and the integral at the right hand side of formula (17) converges. Furthermore, we may project the amplitude (16) on the ℓth partial wave, obtaining

$$a_\ell = \frac{e^{2i\delta_\ell}-1}{2ik} = \frac{g}{\pi}\frac{1}{(\alpha_R + i\beta_R - \ell)(\alpha_R + i\beta_R + \ell + 1)}, \qquad (18)$$

where we write $\lambda = \alpha_R + i\beta_R$ to emphasize that we are now referring to resonances. Next, when the elastic unitarity condition can be applied, we have the following relationship among g, α_R, and β_R:

$$g = -\frac{\pi}{k}\beta_R(2\alpha_R + 1), \qquad (19)$$

and, finally, we obtain:

$$\delta_\ell = \sin^{-1}\frac{\beta_R(2\alpha_R+1)}{\{[(\ell-\alpha_R)^2+\beta_R^2][(\ell+\alpha_R+1)^2+\beta_R^2]\}^{1/2}}. \qquad (20)$$

REMARK. Let us note that the phase shifts of formula (20) do not satisfy the asymptotic behavior, for large values of ℓ, prescribed by formula (14). This derives from the fact that the amplitude given by formula (16), and, accordingly, the phase shifts given by formula (20), are approximations which are faithful only for small values of ℓ. These approximations, however, are acceptable at low energy where a few terms of the partial-wave expansion are sufficient to describe the scattering amplitude.

Representation (20) is useful for the following reasons.

(i) At fixed energy it gives several phase shifts at different values of ℓ, with an acceptable approximation for small values of ℓ.

(ii) α_R and β_R depend on the energy E: i.e., we have a pole trajectory; when $\alpha_R(E)$ equals an integer ℓ, and $\beta_R(E)$ is very small, we have $\sin\ \delta_\ell \simeq 1$, i.e., a resonance.

(iii) Representation (20) can describe, in principle, a sequence of resonances in various partial waves.

Next, if we assume that the colliding particles are spinless bosons (e.g., α particles in α-α collision), then the scattering amplitude must be symmetrized. Therefore, instead of approximation (16), we must write the following one:

$$f(E,\theta) \simeq \frac{g(E)}{\sin\ \pi\lambda(E)}\left[\frac{P_\lambda(\cos\ \theta) + P_\lambda(-\cos\ \theta)}{2}\right], \qquad (21)$$

and, consequently,

$$\delta_\ell = \sin^{-1}\left\{\frac{1+(-1)^\ell}{2}\frac{\beta_R(2\alpha_R+1)}{\{[(\ell-\alpha_R)^2+\beta_R^2][(\ell+\alpha_R+1)^2+\beta_R^2]\}^{1/2}}\right\}. \qquad (22)$$

Approximation (21) fails at $\theta=0$ and $\theta=\pi$, and, in view of the combination of $P_\lambda(\cos\theta)$ and $P_\lambda(-\cos\theta)$, the angular pattern showed by approximation (21) is symmetric.

Coming back to formula (18), and expanding the term $\lambda(E)=\alpha_R(E)+i\beta_R(E)$ in Taylor's series in the neighborhood of the resonance energy, we can derive an estimate of the resonance width Γ_R, i.e.,

$$\Gamma_R = \frac{2\beta_R(d\alpha_R/dE)}{(d\alpha_R/dE)^2 + (d\beta_R/dE)^2}. \qquad (23)$$

However, Γ_R should not be identified with the width Γ of the observed peak of the cross section (see below at the end of this section, and Sec. V). We can now give the following physical interpretation of the term β_R. The resonance is unstable for the leakage of particles tunneling across the centrifugal barrier. Therefore the probability of finding the particles inside a given sphere must decrease with time. The only possibility of keeping up with the loss of probability is to introduce a source somewhere. The source can be provided by the complex centrifugal barrier. The condition for the source to be emitting is just to take $\text{Im}\ \lambda \equiv \beta_R$ positive [see also Eq. (24) below].

We now focus on a peculiar feature associated with nonlocal potentials: in addition to poles located in the first quadrant (i.e., $\text{Im}\ \lambda > 0$), we have also poles located in the fourth quadrant (i.e., $\text{Im}\ \lambda < 0$), which describe the antiresonances. In order to achieve a better understanding of this point, let us consider the continuity equation, which reads [see also Eq. (95) of I]:

$$\frac{\partial w}{\partial t} + \boldsymbol{\nabla}\cdot\mathbf{j} = 2w\ \text{Im}\ \mathcal{U}_{\text{eff}}, \qquad (24)$$

where $w=\chi^*\chi$, χ being the wave function [see also Eq. (4)], $\mathbf{j}$ is the current density: i.e., $\mathbf{j}=i\{\chi\boldsymbol{\nabla}\chi^* - \chi^*\boldsymbol{\nabla}\chi\}$, and $\mathcal{U}_{\text{eff}}$ is the sum of the potential and of the centrifugal term. In the case of local potentials, which do not depend on the

angular momentum, the contribution to Im $\mathcal{U}_{\rm eff}$ comes only from the extension of the centrifugal term to complex-valued angular momentum. The resonances are precisely related to this term. When the potential is nonlocal, and therefore depends on the angular momentum, a contribution to Im $\mathcal{U}_{\rm eff}$ comes also from the potential when the angular momentum is extended to complex values. This contribution cannot be in any way related to the centrifugal barrier, and therefore it cannot be connected to resonances. It rather derives from nonlocality and, accordingly, from the presence of exchange forces which generates the antiresonances (see I). In this case the probability of finding the scattered particle inside a given sphere increases with time. The only possibility of keeping up with this increase of probability is to introduce a negative source, i.e., a pole singularity with Im $\lambda<0$. This term cannot in any way be connected to a (metastable) state; however, we still have a dispersion in energy according to the uncertainty principle. We speak in this case of *time advance* instead of *time delay*, which is proper of the resonance. Analogously, we have a connection between dispersion in angle and dispersion in angular momentum. In fact, let us remark that the antiresonances are a typical quantum-mechanical effect due to the exchange forces. Then, proceeding exactly as in the case of resonances, and denoting the poles in the fourth quadrant by $\lambda=\alpha_A-i\beta_A$, $\beta_A>0$, we have in the neighborhood of an antiresonance:

$$\delta_\ell = \sin^{-1}\frac{-\beta_A(2\alpha_A+1)}{\{[(\ell-\alpha_A)^2+\beta_A^2][(\ell+\alpha_A+1)^2+\beta_A^2]\}^{1/2}}, \tag{25}$$

or, in the case of identical scalar particles,

$$\delta_\ell = \sin^{-1}\left\{\frac{1+(-1)^\ell}{2}\frac{-\beta_A(2\alpha_A+1)}{\{[(\ell-\alpha_A)^2+\beta_A^2][(\ell+\alpha_A+1)^2+\beta_A^2]\}^{1/2}}\right\}. \tag{26}$$

Adding the contributions of poles lying in the first and fourth quadrant, we have

$$\delta_\ell = \sin^{-1}\left\{\frac{\beta_R(2\alpha_R+1)}{\{[(\ell-\alpha_R)^2+\beta_R^2][(\ell+\alpha_R+1)^2+\beta_R^2]\}^{1/2}}\right\}+\sin^{-1}\left\{\frac{-\beta_A(2\alpha_A+1)}{\{[(\ell-\alpha_A)^2+\beta_A^2][(\ell+\alpha_A+1)^2+\beta_A^2]\}^{1/2}}\right\}, \tag{27}$$

and, in the case of identical scalar particles, we obtain

$$\delta_\ell = \sin^{-1}\left\{\frac{1+(-1)^\ell}{2}\frac{\beta_R(2\alpha_R+1)}{\{[(\ell-\alpha_R)^2+\beta_R^2][(\ell+\alpha_R+1)^2+\beta_R^2]\}^{1/2}}\right\}+\sin^{-1}\left\{\frac{1+(-1)^\ell}{2}\frac{-\beta_A(2\alpha_A+1)}{\{[(\ell-\alpha_A)^2+\beta_A^2][(\ell+\alpha_A+1)^2+\beta_A^2]\}^{1/2}}\right\}. \tag{28}$$

Finally, we recall the expression of the total cross section in terms of phase shifts

$$\sigma_{\rm tot} = \frac{4\pi}{k^2}\sum_{\ell=0}^{\infty}(2\ell+1)\sin^2\delta_\ell. \tag{29}$$

In principle, one could try to introduce an estimate of the width of the antiresonances in a form similar to that followed in the case of resonances. In other words we could expand in Taylor's series the term $\lambda(E)=\alpha_A(E)-i\beta_A(E)$, in the neighborhood of the antiresonance energy. These widths should be inversely proportional to the time advance of the outgoing flux. But, while the resonances produce sharp peaks in the cross section and the width of the peaks is well defined and could be properly estimated, this is not the case for the antiresonances. The contribution of the antiresonances to the cross section does not produce sharp peaks and, correspondingly, the width of the antiresonances is ill defined; instead, the antiresonances are responsible for the asymmetry of the cross-section peaks (see Sec. V for phenomenological analysis and examples). Moreover, we want to remark that in the present procedure we can separate neatly the contribution of the resonance from that of the antiresonance and, accordingly, the time delay from the time advance. Resonances and antiresonances are both described in terms of pole singularities, *but acting at different values of energy*. It follows that the interference effect between these terms appears negligible, as will be shown phenomenologically in Sec. V. In view of the difficulty of defining an *antiresonance width* Γ_A, there remains the problem of finding an estimate of the *total* width Γ of the observed (experimental) resonance peak, which is larger than Γ_R in view of the distorting effect of the antiresonance. This problem will be analyzed and discussed in connection with the phenomenological analysis in Sec. V.

IV. FROM RESONANCES TO SURFACE WAVES

Let us first consider the case of Yukawian local potentials, which are represented by a spherically symmetric function on $\mathbb{R}^3$ of the following form: $V(r)=1/r\int_{\mu_0}^{+\infty}e^{-\mu r}\sigma(\mu)d\mu$, $(\mu_0>0)$. We then recall the main properties of the pole trajectories generated by this class of potentials. At negative values of the energy $E=k^2$, the poles $\lambda_n(k)$ lie on the real axis of the λ-plane, and describe bound states. The bound-state wave function belongs to $L^2(0,+\infty)$. Further, these states are

stable and, accordingly, they are described either by poles lying on the imaginary axis of the upper half of the k plane (i.e., Re $k=0$) or by poles located on the real axis of the λ plane (i.e., Im $\lambda=0$): their lifetime is infinite. Increasing the energy, the poles in the λ plane move to the right. This is nothing but the familiar fact that the binding energies of the corresponding bound states of different angular momenta must decrease with increasing ℓ. At positive energy $E=k^2$, the poles $\lambda_n(k)$ enter the first quadrant of the complex λ plane: at those values where Re $\lambda_n(k)$ cross an integer ℓ and correspondingly Im $\lambda_n(k)$ is small, we have a resonance. The lifetime of the latter is inversely proportional to Im $\lambda_n(k)$. As the energy increases, the trajectory could, in principle, describe several resonances: each of them corresponding to the crossing of Re $\lambda_n(k)$ through an integer value ℓ. We could thus have several resonances lying on the same trajectory. But, as we shall show below, this is not the case. In fact, one can show numerical examples of trajectories produced by Yukawian potentials that leave very soon the real λ axis, then turn back toward the left half of the λ plane, and do not exhibit an interpolation of resonances [9]. Furthermore, it can be proved [5,9] that each trajectory, produced by the Yukawian potential, necessarily turns back toward the left half of the λ plane. Therefore, if a pole trajectory $\lambda_n(k)$, moving with positive derivative d Re $\lambda_n(k)/dk$, goes through an integer value ℓ [i.e., Re $\lambda_n(k)=\ell$] and produces a resonance, then, after having turned back to the left, it must necessarily pass through the same integer value ℓ, but now with negative derivative. This latter crossing is not associated with a time delay, but with an advance of the outgoing wave. Thus the peak in the cross section is not a resonance, but comes from the downward passage of the phase shift through $\pi/2$, i.e., it corresponds to an antiresonance. Let us now suppose that a pole trajectory $\lambda_n(k)$, moving with positive derivative d Re $\lambda_n(k)/dk$, crosses several integer values ℓ and describes a sequence of resonances, ordered according to the increasing values of the angular momentum. Then, the same trajectory, after having turned back to the left half of the λ plane, should necessarily describe the corresponding antiresonances in inverse order. One would have at a smaller value of the energy the antiresonances which correspond to the resonances with higher angular momentum. To an ordered sequence of resonances (the order being given by the angular momentum) it would correspond a sequence of antiresonances ordered inversely. This is manifestly contradictory. We can thus conclude that it is not possible to describe with a pole trajectory $\lambda_n(k)$ the ordered sequences of resonances and antiresonances within the framework of the Yukawian potentials.

Therefore, if we want to describe the ordered sequences of resonances and antiresonances, like those produced by rotational bands, we are forced to refer to a larger class of potentials, like the nonlocal ones, introduced previously. As we have seen, this class of potentials admit poles in the fourth quadrant, which are proper for describing antiresonances in view of the fact that their imaginary part is negative, and therefore can describe a time advance instead of a time delay.

In conclusion, we have poles in the first quadrant of the λ plane, whose trajectories describe ordered sequence of resonances, and poles in the fourth quadrant whose trajectories describe ordered sequence of antiresonances. The locations of the poles lying in the first quadrant have an imaginary part that increases with energy, and this behavior corresponds to the increase of the widths of the rotational resonances. The trajectories of these poles keep moving to the right, and not necessarily should turn back to the left. In this evolution we pass from a pure quantum-mechanical effect to semiclassical effects, which can be described in terms of surface waves, as we shall explain below.

As the energy increases, inelastic and reaction channels open: the scenario drastically changes. The elastic unitarity condition does not hold anymore, and the target may now be thought of as a ball partially or totally opaque at the center, and with a semitransparent shell at the border. Accordingly, the potential acquires an imaginary part. The structure of the singularities becomes much more complicated than in the one-channel case. In fact, the structure of the singularities is a superposition of cuts starting at every threshold E_{γ_i}, γ_i labeling the channels. In spite of these difficulties, we can still, roughly speaking, continue the trajectory of the pole in the complex angular momentum plane with the only caution of avoiding the use of the elastic unitarity condition (19). Moreover, when the energy increases, the effects of the exchange forces, which are a pure quantum effect, tend to vanish. Therefore we can still retain approximation (16), which represents the elastic scattering, but now its physical interpretation must be appropriately modified. We have seen that the width of the rotational resonances increases with the energy; accordingly, $\beta_R \equiv$ Im λ increases. It follows that when $\alpha_R \equiv$ Re λ crosses an integer value, but β_R is not much smaller than one, we do not observe sharp peaks in the cross section since $|\sin(\pi\alpha_R+i\beta_R)|^{-1} \simeq \exp\{-\pi\beta_R\}$: we have diffractive effects. These phenomena can be very well described by returning to formula (16), which can now be conveniently written in the following form:

$$f(E,\theta) \simeq C(E) P_{\lambda(E)}(-\cos\theta). \tag{30}$$

In this way the amplitude is factorized into two terms: the first one, $C(E)$, gives the amplitude at $\theta=\pi$ as a function of E [in fact, $P_\lambda(1)=1$]; the second factor describes the backward angular distribution at fixed E. This second term may be easily interpreted by recalling the asymptotic behavior of $P_\lambda(-\cos\theta)$ for large values of $|\lambda|$. In fact, it holds [7] that, for $0<\theta<\pi$,

$$P_\lambda(-\cos\theta) \propto \frac{e^{-i[(\lambda+1/2)(\pi-\theta)-\pi/4]} + e^{i[(\lambda+1/2)(\pi-\theta)-\pi/4]}}{(2\pi\lambda\sin\theta)^{1/2}}. \tag{31}$$

These exponentials correspond to the surface waves excited at the periphery of the target by the grazing rays. These rays undergo at the point of tangency a splitting: one ray leaves the target (which is supposed, for simplicity, to be a sphere) tangentially, while the other one propagates along the edge; finally, if the blackbody limit is not yet reached, we may also have a refracted ray which pen-

etrates the weakly absorbing region. Moreover, the surface ray undergoes at any point the same splitting described above; also the refracted ray, after emerging at the surface, undergoes the same splitting, sending off tangential rays. However, these latter rays are in phase and unidirectional only in the direct forward and backward directions. The factor $(\sin\theta)^{-1/2}$ describes precisely this focusing effect at $\theta=0$, and $\theta=\pi$.

In order to have the exact expression of the surface waves, excited by the grazing rays at the periphery of the target, we must introduce the surface angle $\theta_m^{(S_\pm)}$ in place of the scattering angle θ. The relationship is as follows:

$$\theta_m^{(S_+)} = \theta + 2\pi m \quad (m = 0, 1, 2, \ldots), \tag{32a}$$

$$\theta_m^{(S_-)} = 2\pi - \theta + 2\pi m, \tag{32b}$$

where $\theta_m^{(S_+)}$ refers to the counterclockwise traveling rays, while $\theta_m^{(S_-)}$ corresponds to the clockwise ones. By using formula (31) it can be shown that the Legendre function $P_\lambda(-\cos\theta)$ can be generated by the superposition of exponentials of the form $e^{i\lambda\theta_m^{(S_\pm)}}$, representing surface waves creeping around the target [10]. Coming back to formula (16), we recall that the latter is logarithmically divergent at $\theta=0$, but it is not at $\theta=\pi$. This different behavior is in agreement with the fact that the damping factor of the surface waves is given by $e^{-\mathrm{Im}\,\lambda\theta_m^{(S_\pm)}}$. Then, forwards, where the damping factor is nearly equal to 1, an infinity of creeping waves contribute to the total amplitude: we have a divergence. On the contrary, the creeping wave approximation works better backwards, since $\mathrm{Im}\,\lambda\ \theta_m^{(S_\pm)}$ is larger.

In order to evaluate the term $C(E)$, let us suppose that the blackbody limit has been reached. Then the grazing ray at the tangency point will split into two branches only: a surface ray which describes a geodesic around the target, and another ray which leaves the surface tangentially. The point where diffraction takes place may be regarded as an interaction vertex, characterized by a coupling constant, while the line joining two vertices may be regarded as a propagator. The coupling constants are the diffraction coefficients; the propagator, for a surface ray describing an arc length $\theta_m^{(S_\pm)}$, takes the form $e^{i\lambda\theta_m^{(S_\pm)}}$. Next, we suppose that the so-called *localization principle* holds true: the phenomena which occur for large energy, on the periphery of the interaction region, are independent of the inner structure of the target. Therefore we take for $\mathrm{Im}\,\lambda$ (which characterizes the propagator), as well as for the coupling constant (the diffraction coefficient) an energy dependence as the one calculated for a wholly transparent sphere [11]. Then, the formula for the cross section at $\theta=\pi$ is given by [11,4]

$$\frac{\pi}{k^2}\left(\frac{d\sigma}{d\Omega}\right)_{\theta=\pi} = C_0 k^{-4/3} e^{-ck^{1/3}} \quad (c = \mathrm{const}), \tag{33}$$

where C_0 is a constant beyond the blackbody limit. Before reaching the blackbody limit, the grazing rays may undergo a critical refraction, penetrate the weakly absorbing region, and then emerge after one or two shortcuts (see Fig. 2). In this case C_0 is not a constant since it must take into account the contributions of various components: the diffracted rays which do not undergo any shortcut and the critically refracted rays which take one or two shortcuts before emerging. These various contributions interfere, producing an oscillating pattern. But, as the momentum increases, the radius of the central opaque core increases too, and the shortcuts are progressively suppressed; therefore the amplitude of these oscillations is damped and tends to vanish towards the blackbody limit. In order to fit this oscillating pattern, we use a function of the following form: $[1+A\,\sin(\omega k+\phi)]$. Accordingly, we shall fit the experimental data (see Sec. V) with the following formula:

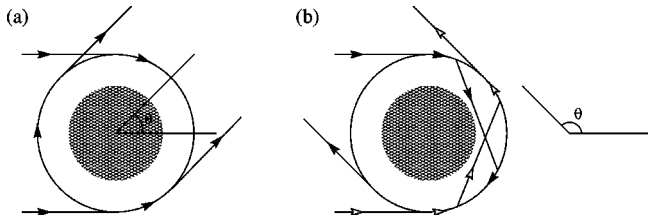

FIG. 2. Diffracted rays emerging along the direction θ. (a) Without taking any shortcut. (b) Taking one shortcut.

$$\frac{\pi}{k^2}\left(\frac{d\sigma}{d\Omega}\right)_{\theta=\pi} = C_0 k^{-4/3} e^{-ck^{1/3}}[1 + A\,\sin(\omega k + \phi)]. \tag{34}$$

Let us finally note that the complex angular momentum poles which are connected to resonances and those which are associated with surface waves present remarkable differences. We can, indeed, speak of two different classes of poles [9]. The poles of the first class are located near the real axis of the complex λ plane, and are associated with resonances. The poles of the second class lie along a line which is nearly parallel to the imaginary axis: they are insensitive to the behavior of the potential in the inner region, and are associated with surface waves [9]. Further, the poles of the second class move nearly parallel to the real axis when the energy increases.

To these different classes of poles we can associate two different physical models: vortices and surface waves produced by diffracted rays. In order to summarize rapidly the hydrodynamical model of the vortices, we move back to the expression of the current density, introduced in Sec. III: i.e., $\mathbf{j}=i\{\chi\boldsymbol{\nabla}\chi^*-\chi^*\boldsymbol{\nabla}\chi\}$, where χ is the wave function (see also Ref. [1]). Assuming a semiclassical approximation, we write $\chi=(A/\sqrt{2})e^{i\Theta}$($A$=const); accordingly, we have $\mathbf{j}=A^2\boldsymbol{\nabla}\Theta$. Then we introduce a velocity field $\mathbf{v}$, regarding Θ as a velocity potential in the hypothesis of irrotational flow: $\mathbf{v}=\boldsymbol{\nabla}\Theta$. First, we represent the incoming beam as an irrotational flow streaming around the target. Then the trapping proper of the resonance can be depicted as a rotational flow ω given by $\omega=\boldsymbol{\nabla}\times\mathbf{v}$.

The diffracted rays which generate surface waves are due to a completely different process. Regarding the diffraction as an obstacle problem in a Riemannian space with boundary, we can consider the edge of the diffracting body as the boundary of the ambient space. Then the determination of the geodesics by their initial tangent (Cauchy problem) is not

unique: when a ray grazes a boundary surface, the ray splits in two parts, one keeps going as an ordinary ray, whereas the other part travels along the surface. This is precisely the mechanism which generates diffracted rays and surface waves [10]. We thus call the first class of poles associated with vortices, and representing resonances, Regge poles; while the name Sommerfeld poles is reserved for the second class of poles, in view of the fact that they have been discovered by Sommerfeld [8] in connection with the diffraction of radio waves around the Earth.

V. PHENOMENOLOGICAL ANALYSIS

A. Rotational band in α-α elastic scattering

The α-α elastic scattering is certainly a good laboratory for testing the theory, since it is a system of two identical spinless particles which clearly displays rotational bands. The data, which we analyze, are the experimental phase shifts, taken from Refs. [12–16], the range of energies extending up to 40 MeV in the center of mass system. In this range of energies, in addition to the elastic channel that we here consider [notice that to obtain formula (28) the unitary elastic condition was assumed to hold], there are several other inelastic and reaction channels: for instance, the reaction channel $p+\mathrm{Li}^7$, whose threshold energy is 17.25 MeV [17]. Therefore, the experimental phase shifts contain nonvanishing imaginary parts, and even their real part is affected by these channels. For this reason considering only the real part of the experimental phase shifts, as we do in the following, is admittedly an approximation. Nevertheless, we assume that the effects of the nonelastic channels on the real part of the experimental phase shifts is negligible within the considered energy range, and we compare the phase shifts computed by the theory presented in the previous sections with the real part of the experimental phase shifts. Finally, instead of fitting the differential cross section, we prefer to fit the phase shifts so that the action of the Coulomb potential can be subtracted. However, in connection with the interference effects related to the Coulomb subtraction, the following two remarks should be made.

(i) In view of the long range of the Coulomb force, the exchange part of the Coulomb interaction does not affect greatly the scattering wave function (see Ref. [18] and the references therein) [19].

(ii) For the sake of preciseness, one should distinguish the *quasinuclear* phase shifts δ_ℓ from the *purely nuclear* phase shifts δ_ℓ^*, which are those associated with the scattering between the same particles, with the same strong properties but without the Coulomb interaction [21]. It is rather intuitive, and can be rigorously proved [21,22], that they differ by quantities proportional to the Sommerfeld parameter $\eta = Z_1 Z_2 e^2/\hbar v$. Even though η can be significantly large at low energies, nevertheless, this fact does not prevent the phase shifts δ_ℓ from being treated as corresponding to a short range potential and retaining the main properties of interest for our analysis. The reader interested in a rigorous mathematical analysis of the Coulomb effects at $k=0$ is referred to Ref. [23], where it is proved that an additional Coulomb potential does not affect the general properties of the Regge's trajectories except for their threshold behavior.

The functions $\alpha_R(E)$, $\beta_R(E)$, $\alpha_A(E)$, and $\beta_A(E)$ in formula (28) are parametrized as follows:

$$\alpha_R(E)[\alpha_R(E)+1] = 2IE + \alpha_0, \tag{35a}$$

$$\beta_R(E) = b_1\sqrt{E}, \tag{35b}$$

$$\alpha_A(E) = a_1 E^{1/4}, \tag{35c}$$

$$\beta_A(E) = g_0(1 - e^{-E/E_0}) + g_1 E + g_2 E^2, \tag{35d}$$

where $I=\mu R^2$ is the moment of inertia, μ is the reduced mass, R is the interparticle distance, and E is the center of mass energy. Formula (35a) for the resonant component $\alpha_R(E)$ simply gives the angular momentum of the two-particle system viewed, in first approximation, as a rotator; formula (35b) states for $\beta(E)$ a growth which is fast for low energy, but slower for higher energy; this behavior suits the analysis done in Sec. IV concerning the evolution of the resonances into surface waves for sufficiently large energy. For what concerns $\beta_A(E)$ in formula (35d), the role of the exponential term is just to make a smooth, though rapid, transition of $\beta_A(E)$ from zero to the constant g_0, so as to have a regular behavior at very low energy. Unfortunately, a model which prescribes the growth properties of $\alpha_A(E)$ and $\beta_A(E)$ is, at present, missing. This would require a refined theory able to describe the evolution toward semiclassical and classical phenomena. The quantities I, α_0, b_1, a_1, g_0, g_1, and g_2 should be regarded as fitting parameters. In what follows, we will consider phenomena occurring only above threshold; therefore we do not analyze the $\ell=0$ phase shift, which is ruled by the low-energy behavior of the trajectories $\alpha_A(E)$ and $\beta_A(E)$. In particular, the resonance-antiresonance correspondence is missing in the $\ell=0$ phase shift, and to date this makes it difficult to reproduce this phase shift in the framework of our model.

In Fig. 3(a) the fits of the experimental phase shifts, obtained by means of Eq. (28), for $\ell=2,4$ are shown, while Fig. 3(c) shows the effect of the antiresonance on the $\ell=2$ phase shift. The resulting numerical values of the fitting parameters are given in the figure legend. It is clear that the phase shifts obtained by using Eq. (28) reproduce rather well the experimental data. In particular, they are notably better than the ones obtained previously in Ref. [3], where a hard-core model of the repulsive part of the interaction was implemented, and whose phase shifts turned out to be not adequate for representing the nonresonant part of the phase shifts over a sufficient energy range (see also Refs. [14,15]). Table I summarizes the results of the analysis for what concerns the 2^+ and 4^+ resonances. The agreement with the experimental values appears quite good, but for a slight discrepancy in the 2^+ total width Γ. However, as will be discussed later in this section, care must be taken in the interpretation of the resonance widths. It is worth remarking that some experimental indications of a 6^+ state at $E_R \sim 28$ MeV and of an 8^+ state at $E_R \sim 57$ MeV have been reported [24]. Pushing forward our analysis, and computing δ_ℓ from Eq. (28) even for $\ell=6$ and $\ell=8$, we obtain a resonance 6^+ at $E_R \sim 27.2$ MeV, and a 8^+

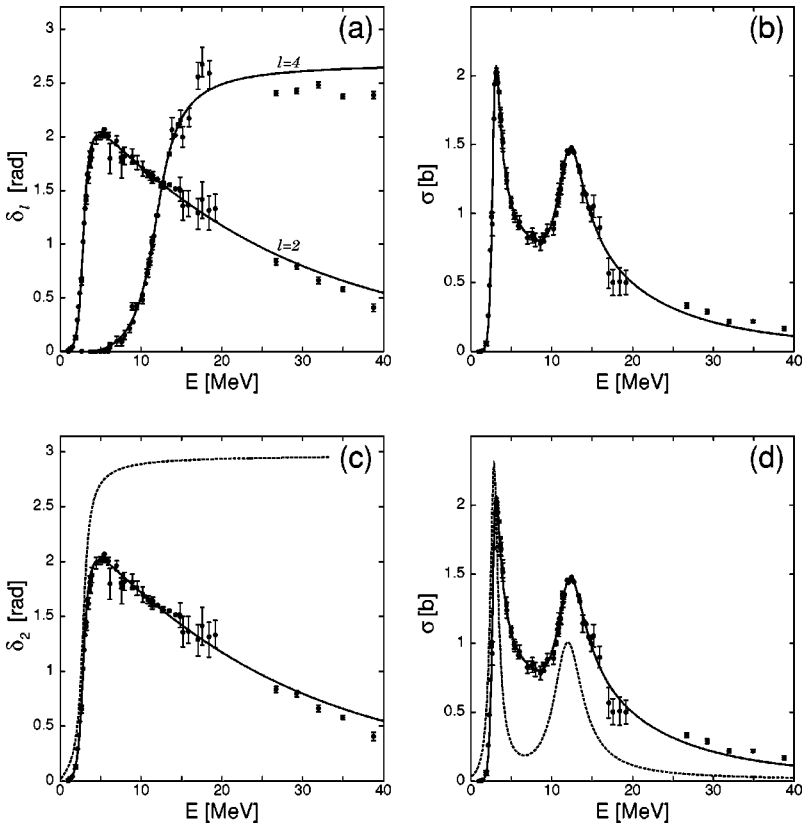

FIG. 3. α-α elastic scattering. (a) Experimental phase shifts for the partial waves $\ell=2$, $\ell=4$, and corresponding fits (solid lines) [see formula (28)], vs the center of mass energy E. Experimental data are taken from Refs. [12–16]. The numerical values of the fitting parameters are (see text): $I=0.76$ $(\mathrm{MeV})^{-1}$, $\alpha_0=1.6$, $b_1=1.06\times10^{-1}$ $(\mathrm{MeV})^{-1/2}$, $a_1=1.03$ $(\mathrm{MeV})^{-1/4}$, $g_0=0.72$, $g_1=-7.5\times10^{-3}$ $(\mathrm{MeV})^{-1}$, $g_2=2.0\times10^{-5}$ $(\mathrm{MeV})^{-2}$, $E_0=4.1$ MeV. (b) Total cross section computed by using the phase shifts in (a) [see formula (29)]. (c) Phase shift for the partial wave $\ell=2$. The solid line indicates the phase shift computed by using formula (28), which takes into account both the resonance and antiresonance terms. The dashed line shows the phase shift computed by using only the resonance term [see formula (22)]. (d) Comparison between the total cross section computed by accounting for both the resonance and antiresonance terms (solid line), and that computed by using only the resonance term (dashed line).

resonance at $E_R\sim47$ MeV. Then, with a single pair of pole trajectories (one for resonances and one for antiresonances) this rotational band of resonances can be fitted quite accurately.

From formula (29) the total cross section can be computed from the phase shifts of Fig. 3(a): the result is shown in Fig. 3(b), while in Fig. 3(d) the total cross sections computed with and without the antiresonance term are compared.

The analysis of the total cross section arouses the issue regarding the definition of the resonance parameters, in particular of the width Γ of the resonance. The extraction of the resonance parameters is model dependent, and many ways to proceed in practice have been presented in the literature (see, for instance, Refs. [25,26] and the references therein). The estimate of Γ presents several difficult questions in the framework of the present theory as well as in the Breit-Wigner formalism. In both theories the main difficulty derives from the effect of the antiresonance which deforms the bell-shaped symmetry of the resonance peak. Further, we must note the following.

(i) In the present theory, formula (23) provides an estimate of the pure resonance width Γ_R, which must be understood as the width of the resonance in the absence of the antiresonance effect; as explained in Sec. III an analogous estimate for the *antiresonance width* Γ_A is hardly definable.

(ii) In the fit of the experimental cross section within the Breit-Wigner theory, the estimate of Γ is obtained by adding to the pure resonance a background term, which is supposed to be generated by the so-called potential scattering. One obtains a purely phenomenological result.

Reverting to our theory, in order to give a phenomenological estimate of the width Γ, two different situations should be distinguished.

(I) The effect of the antiresonance is a small perturbation to the pure resonance (see, for instance, the leftmost reso-

TABLE I. α-α elastic scattering. In the present work the resonance energy E_R, associated with the angular momentum ℓ, is defined as the energy of the upward $\pi/2$ crossing of the corresponding phase shift $\delta_\ell(E)$. The *purely resonant* Γ_R indicates the width of the resonance peak computed without the antiresonance contribution, while the *total* Γ stands for the width of the resonance peak accounting also for the antiresonance term. $\Delta\mathcal{S}/\mathcal{S}_{\mathrm{Res}}$ indicates the relative increase of skewness of the resonance peak when the antiresonance contribution is added to the pure resonant term; here $\mathcal{S}$ is evaluated by means of $\mathcal{S}_{\mathrm{phen}}$.

J^P	E_R(MeV) (Present work)	E_R(MeV) (Ref. [24])	Γ_R(MeV) Purely resonant	Γ(MeV) Total	Γ(MeV) (Ref. [24])	$\Delta\mathcal{S}/\mathcal{S}_{\mathrm{Res}}$
2^+	3.23	3.27	1.04	2.58	1.50	20.53
4^+	12.6	11.6±0.3	4.33	4.91	4.0±0.4	2.35

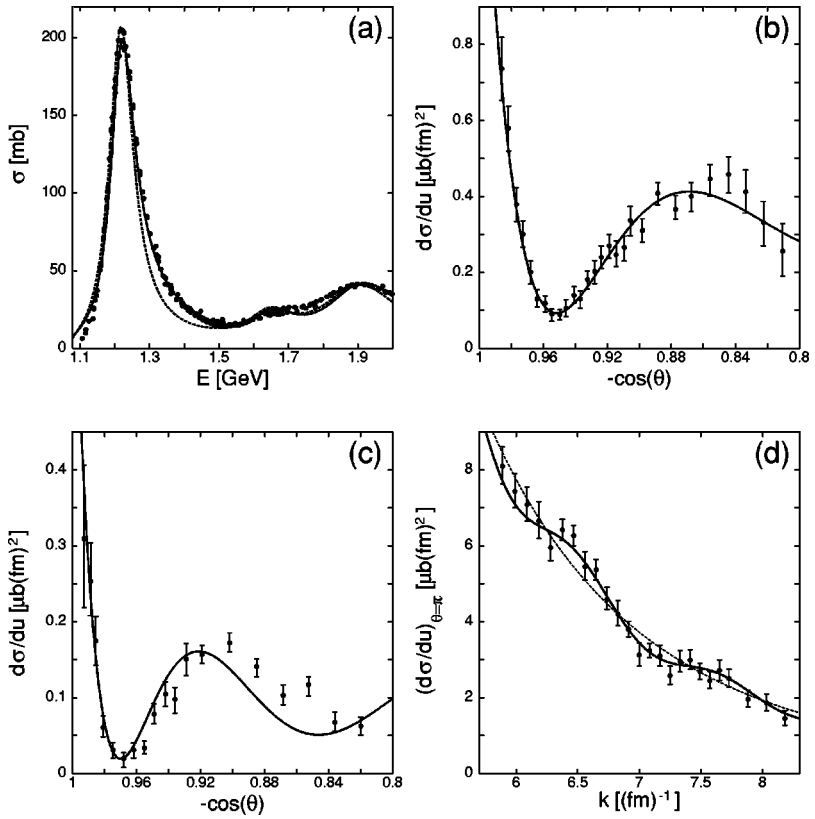

FIG. 4. π^+-p elastic scattering. (a) Total cross section. The experimental data (dots) are taken from Ref. [31]. The solid line indicates the total cross section computed by means of Eq. (39), and taking into account the contributions of both the resonance and antiresonance poles generating $\delta_\ell^{(+)}$ [formula (40)], and the resonance pole generating $\delta_\ell^{(-)}$. The dashed line shows the total cross section computed by accounting only for the resonance poles generating $\delta_\ell^{(+)}$ and $\delta_\ell^{(-)}$, respectively. The fitting parameters are [see Eqs. (40), (41), and (42a)–(42f)] $a_0^{(+)}=6.89\times10^{-1}$, $a_1^{(+)}=9.2\times10^{-7}$ $(\mathrm{MeV})^{-2}$, $b_1^{(+)}=9.0\times10^{-5}$ $(\mathrm{MeV})^{-1}$, $b_2^{(+)}=1.4\times10^{-7}$ $(\mathrm{MeV})^{-2}$, $c_0=-0.5$, $c_1=5.0\times10^{-7}$ $(\mathrm{MeV})^{-2}$, $g_0=2.0\times10^{-6}$ $(\mathrm{MeV})^{-2}$, $g_1=3.0\times10^{-12}$ $(\mathrm{MeV})^{-4}$, $a_1^{(-)}=6.4\times10^{-7}$ $(\mathrm{MeV})^{-2}$, $b_1^{(-)}=1.25\times10^{-4}$ $(\mathrm{MeV})^{-1}$. (b) Differential cross section vs $(-\cos\theta)$, at $s=E^2=10.66$ $(\mathrm{GeV})^2$. The experimental data (dots) are taken from Ref. [27]. The solid line shows the differential cross section computed by means of Eq. (43). The fitting parameters are Re $\lambda=7.1$, Im $\lambda=1.3$, $B_0=1.61$ μb $(\mathrm{fm})^2$, $B_1=8.0\times10^{-4}$ μb $(\mathrm{fm})^2$. (c) Differential cross section vs $(-\cos\theta)$, at $s=E^2=14.04$ $(\mathrm{GeV})^2$. The fitting parameters are: Re $\lambda=9.2$, Im $\lambda=1.2$, $B_0=0.778$ μb $(\mathrm{fm})^2$, $B_1=1.6\times10^{-5}$ μb $(\mathrm{fm})^2$. (d) Differential cross section at $\theta=\pi$ vs k. The experimental data (dots) are taken from Ref. [28]. The solid line shows the differential cross section computed by means of Eq. (34). The fitting parameters are $C_0=1.85\times10^6$ μb $(\mathrm{fm})^{2/3}$, $c=5.5$ $(\mathrm{fm})^{1/3}$, $A=-9.3\times10^{-2}$, $\omega=5.4$ fm, $\phi=0.84$. The dashed line shows the differential cross section computed by means of formula (33), in which the oscillating term is absent.

nance peak in Fig. 4(a) in connection with the π^+-p elastic scattering). This means that the reference baseline of the pure resonance peak and that of the observed cross section (comprising both resonance and antiresonance) coincide within a good approximation.

In this case we can proceed operatively as follows. First, from formula (23) we obtain the estimate of Γ_R. Then, from the plot of the cross section generated by only the pure resonant term, i.e., obtained by using only the pole singularity lying in the first quadrant of the λ plane, we can recover the reference baseline of this almost symmetric bell-shaped distribution by equating its second central moment to the the value of Γ_R [evaluated by means of Eq. (23)]. Next, keeping fixed this baseline, we evaluate the second central moment of the distribution which fits the experimental cross-section peak (i.e., accounting also for the antiresonant term). We can take as an estimate of the total width Γ the value of this second moment. As a measure of the degree of asymmetry of the resonance peak, which can be ultimately ascribed to the composite structure (nonelementariness) of the interacting particles, we take the statistical skewness $\mathcal{S}_{\mathrm{stat}}$ of the distribution, defined as $\mathcal{S}_{\mathrm{stat}}=\mu_3/\mu_2^{3/2}$, where μ_2 and μ_3 are, respectively, the second and third central moments of the distribution (see Table II for the numerical values related to the π^+-p elastic scattering). This procedure works reasonably well as far as the asymmetry of the resonance peak is not too large and can be regarded as a small perturbation of the pure resonance effect, as in the case of the $\Delta(\frac{3}{2},\frac{3}{2})$ resonance in the π^+-p elastic scattering, which will be treated in the following subsection.

(II) The asymmetry of the bell-shaped peak is very large, and the antiresonance effect cannot be regarded as a small perturbation to the pure resonance [see Figs. 3(b) and 3(d) in connection with the α-α elastic scattering]. In this case the increase of the cross section corresponding to the downward crossing of $\pi/2$ of the phase shift is relevant and deforms considerably the shape of the pure resonant peak. Moreover, the reference baseline of the pure resonance peak and that of

the observed experimental cross section differ significantly, so that a statistical approach as the one described in the previous case (I) cannot be adopted. We are forced to follow a more pragmatic attitude. Since the asymmetry due to the antiresonance effect sets in just after the resonance maximum, we can regard Γ as the full width at half maximum of the resonance peak, like in the Breit-Wigner theory. From the plot of the pure resonance cross section we obtain a bell-shaped distribution whose full width at half maximum agrees with the value of Γ_R evaluated by formula (23). Then we can give an estimate of the total width Γ by evaluating the full width at half maximum of the curve fitting the experimental cross section (i.e., including both resonance and antiresonance terms). In this case the asymmetry of the resonance peak can be estimated by using a *phenomenological skewness* $\mathcal{S}_{\rm phen}$, defined as follows: first we compute the difference between the two half-maximum semiwidths, measured with respect to the energy of resonance E_R; then the degree of asymmetry $\mathcal{S}_{\rm phen}$ is defined as the ratio between this value and the full width Γ (see Table I for numerical values related to the α-α elastic scattering).

B. Resonances and surface waves in π^+-p elastic scattering

In the analysis of the π^+-p scattering the spin of the proton must be taken into account. Therefore, we start recalling rapidly the main formulas for the scattering amplitude in the case of spin-0–spin-$\frac{1}{2}$ collision. In particular, we have the spin-non-flip amplitude and the spin-flip amplitude, which, respectively, read

$$f(k,\theta)=\frac{1}{2ik}\sum_{\ell=0}^{\infty}[(\ell+1)(\mathbb{S}_\ell^{(+)}-1)+\ell(\mathbb{S}_\ell^{(-)}-1)]P_\ell(\cos\theta), \tag{36a}$$

$$g(k,\theta)=\frac{1}{2k}\sum_{\ell=0}^{\infty}(\mathbb{S}_\ell^{(+)}-\mathbb{S}_\ell^{(-)})P_\ell^{(1)}(\cos\theta), \tag{36b}$$

where $P_\ell^{(1)}(\cos\theta)$ is the associated Legendre function, and

$$\mathbb{S}_\ell^{(+)}=e^{2i\delta_\ell^{(+)}}, \tag{37a}$$

$$\mathbb{S}_\ell^{(-)}=e^{2i\delta_\ell^{(-)}}, \tag{37b}$$

$\delta_\ell^{(\pm)}$ being the phase shift associated with the partial wave with total angular momentum $j=\ell\pm\frac{1}{2}$. The differential cross section is given by

$$\frac{d\sigma}{d\Omega}=|f|^2+|g|^2, \tag{38}$$

if the proton target is unpolarized, and if the Coulomb scattering is neglected, as it is admissible at energy sufficiently high. Let us note that the Sommerfeld parameter $\eta=e^2/\hbar v$ at $E\simeq 1200$ MeV [close to the energy of the $\Delta(\frac{3}{2},\frac{3}{2})$ resonance] is of the order of 0.04. Next, integrating over the angles and taking into account the orthogonality of the spherical harmonics, we obtain for the total cross section the following expression:

$$\sigma_{\rm tot}=\frac{2\pi}{k^2}\sum_{j,\ell}(2j+1)\sin^2\delta_{\ell,j}, \tag{39}$$

where $j=\ell\pm\frac{1}{2}$, $\delta_{\ell,j}=\delta_{\ell,\ell\pm1/2}$, $\delta_{\ell,\ell+1/2}\equiv\delta_\ell^{(+)}$, $\delta_{\ell,\ell-1/2}\equiv\delta_\ell^{(-)}$.

We put at the center of our analysis the $\Delta(\frac{3}{2},\frac{3}{2})$ resonance. It is considered the first member of a family of resonances whose J^P values are precisely given by $\frac{3}{2}^+$, $\frac{7}{2}^+$, $\frac{11}{2}^+$, $\frac{15}{2}^+$, $\frac{19}{2}^+$. It has been suggested [29] that this sequence could correspond to an even rotational band of the proton states whose angular momentum is given by $L=0^+,2^+,4^+,6^+,8^+$. We could as well have an odd rotational band of proton states with angular momentum: $L=1^-,3^-,\ldots$. But, in the π^+-p elastic scattering, we observe only one resonance with $J^P=\frac{1}{2}^-$, which could correspond to the first member (i.e., $L=1^-$) of this odd rotational band [30] (see Ref. [29]).

Let us now focus on the first family of resonances. In our model they should be fitted by the trajectory of one pole lying in the first quadrant of the complex angular momentum plane. But, since the proton and the pion are composite particles, the antiresonances should play a role. Accordingly, we should add the contribution of a pole in the fourth quadrant of the complex angular momentum plane. Furthermore, since the spin of the proton is fixed, we limit ourselves to perform the analytic continuation of the partial waves from integers to complex values of the angular momentum ℓ. Therefore, we shall fit the resonances belonging to the family whose first member is $\Delta(\frac{3}{2},\frac{3}{2})$, by writing for $\delta_{\ell,\ell+1/2}\equiv\delta_\ell^{(+)}$ the following expression:

$$\delta_\ell^{(+)}=\sin^{-1}\left\{\frac{1-(-1)^\ell}{2}\frac{\beta_R^{(+)}(2\alpha_R^{(+)}+1)}{\{[(\ell-\alpha_R^{(+)})^2+(\beta_R^{(+)})^2][(\ell+\alpha_R^{(+)}+1)^2+(\beta_R^{(+)})^2]\}^{1/2}}\right\}$$
$$+\sin^{-1}\left\{\frac{1-(-1)^\ell}{2}\frac{-\beta_A^{(+)}(2\alpha_A^{(+)}+1)}{\{[(\ell-\alpha_A^{(+)})^2+(\beta_A^{(+)})^2][(\ell+\alpha_A^{(+)}+1)^2+(\beta_A^{(+)})^2]\}^{1/2}}\right\}. \tag{40}$$

(Let us note that the factor $[1-(-1)^\ell]/2$ in formula (40) and in the next formula (41), instead of $[1+(-1)^\ell]/2$, is due to the fact that we interpolate odd values of ℓ.**)**

We can now pass to consider the second family of resonances, whose first member is $\Delta(\frac{1}{2},\frac{3}{2})$. But, as mentioned above, this resonance is the sole member of this sequence which is phenomenologically observed in elastic scattering. We thus introduce a second trajectory of a pole lying in the first quadrant. In view of the small effect of this resonance on the total cross section, we neglect the corresponding antiresonance pole. Then, with obvious meaning of the notations, we write for $\delta_{\ell,\ell-1/2}\equiv\delta_\ell^{(-)}$,

$$\delta_\ell^{(-)} = \sin^{-1}\left\{ \frac{1-(-1)^\ell}{2} \frac{\beta_R^{(-)}(2\alpha_R^{(-)}+1)}{\{[(\ell-\alpha_R^{(-)})^2+(\beta_R^{(-)})^2][(\ell+\alpha_R^{(-)}+1)^2+(\beta_R^{(-)})^2]\}^{1/2}} \right\}. \tag{41}$$

We then fit the total cross section parametrizing $\alpha_R^{(\pm)}$, $\beta_R^{(\pm)}$, $\alpha_A^{(+)}$, and $\beta_A^{(+)}$ as follows:

$$\alpha_R^{(+)} = a_0^{(+)} + a_1^{(+)}(E^2 - E_0^2), \tag{42a}$$

$$\beta_R^{(+)} = b_1^{(+)}\sqrt{E^2 - E_0^2} + b_2^{(+)}(E^2 - E_0^2), \tag{42b}$$

$$\alpha_A^{(+)} = c_0 + c_1(E^2 - E_0^2), \tag{42c}$$

$$\beta_A^{(+)} = g_0(E^2 - E_0^2) + g_1(E^2 - E_0^2)^2, \tag{42d}$$

$$\alpha_R^{(-)} = a_1^{(-)}(E^2 - E_0^2), \tag{42e}$$

$$\beta_R^{(-)} = b_1^{(-)}\sqrt{E^2 - E_0^2}, \tag{42f}$$

where E is the energy in the center of mass frame, and E_0 is the rest mass of the π^+-p system.

Substituting the values $\delta_\ell^{(\pm)}$ [formulas (40), (41), and (42a)–(42f)] in formula (39) we can fit the total cross section (the data are taken from Ref. [31]). The result is shown in Fig. 4(a), where the total cross sections computed with (solid line) and without (dashed line) the antiresonance term are compared (see the figure legend for numerical details). The fit is very satisfactory, and shows with clear evidence the effect of the antiresonance corresponding to the resonance $\Delta(\frac{3}{2},\frac{3}{2})$. The difference between the two curves reveals the composite structure of the interacting particles [32].

In Table II the analysis for family of resonances $\Delta(\frac{3}{2},\frac{3}{2})$, $\Delta(\frac{7}{2},\frac{3}{2})$, $\Delta(\frac{11}{2},\frac{3}{2})$, $\Delta(\frac{1}{2},\frac{3}{2})$ is summarized. In particular we give the energy location, the purely resonant and total widths, and the skewness ascribable to the antiresonance phenomenon. It should be remarked that the values of the $\Delta(\frac{11}{2},\frac{3}{2})$ resonance, which is not visible in Fig. 4(a), have been extrapolated by computing $\delta_{\ell=5}^{(+)}$ with the parameters obtained from the analysis of the $\Delta(\frac{3}{2},\frac{3}{2})$ and $\Delta(\frac{7}{2},\frac{3}{2})$ resonances (see the legend of Fig. 4). It is worth noticing from the last column in Table II that the degree of asymmetry associated with the resonance peaks decreases notably when the angular momentum ℓ increases. This behavior was expected since the asymmetry of the resonance peaks is due to the antiresonances, whose effect tends to disappear as ℓ increases (see also Table I for a similar behavior in connection with the α-α scattering).

As shown in Fig. 4(a) we can fit the total cross section up to a value of E of the order of 2000 MeV. At higher energy, the elastic unitarity condition is largely violated, and the fitting formula should be modified accordingly. Furthermore, the resonances $\frac{15}{2}^+$ and $\frac{19}{2}^+$ do not display sharp peaks in the total cross section. This means that the resonances evolve into surface waves in the sense described in Sec. IV. At these energies the partial-wave analysis cannot be properly applied, nor has it the meaning to separate the $\delta_\ell^{(+)}$ from the $\delta_\ell^{(-)}$ trajectories. As explained in Sec. IV, we can try two different types of fits: (i) at fixed energy; (ii) at fixed angle, i.e., $\theta = \pi$. We start with the first type of fit. With this in mind we approximate the differential cross section in the backward direction with the following formula:

$$\frac{\pi}{k^2}\frac{d\sigma}{d\Omega} \simeq B_0|P_\lambda(-\cos\,\theta)|^2 + B_1|P_\lambda^{(1)}(-\cos\,\theta)|^2. \tag{43}$$

In formula (43) we introduce the term $B_1|P_\lambda^{(1)}(-\cos\,\theta)|^2$, which gives the contribution to the differential cross section of the spin-flip amplitude [see formulas (36)]. In Figs. 4(b) and 4(c) we present two fits of the differential cross section in the backward angular region $0.8 < -\cos\,\theta < 1.0$, at fixed energy. The fits are satisfactory, and B_1 turns out to be negligible, compared to B_0. Let us moreover note that the values of Reλ obtained by these fits indicate that we do not have resonances at $J^P = \frac{15}{2}^+$ and $J^P = \frac{19}{2}^+$, but backward peaks due to creeping wave effects, which can be described by the Sommerfeld poles, instead of by the Regge's ones.

Finally, in Fig. 4(d) we present a fit at fixed angle $\theta = \pi$. The fit is performed by means of formula (34), derived in Sec. IV. It presents a clear evidence of an oscillating pattern due to the interference of grazing rays which undergo a different number of shortcuts. As the energy increases, the radius of the central core increases too, and the shortcuts are progressively suppressed: the oscillating pattern is damped.

TABLE II. π^+-p elastic scattering. Notice that, in the rightmost column, $\mathcal{S}$ is evaluated by means of $\mathcal{S}_{\rm stat}$. For the other definitions, see the legend of Table I.

J^P	Mass (MeV) (Present work)	Mass (MeV) (Ref. [31])	Γ_R(MeV) Purely resonant	Γ(MeV) Total	Γ(MeV) (Ref. [31])	$\Delta\mathcal{S}/\mathcal{S}_{\rm Res}$
$\frac{3}{2}^+$	1231	1230–1234	84	117	115–125	4.40
$\frac{7}{2}^+$	1941	1940–1960	273	308	290–350	3.80
$\frac{11}{2}^+$	2445	2300–2500	374	410	300–500	3.24
$\frac{1}{2}^-$	1655	1615–1675	147		120–180	

[1] E. De Micheli and G. A. Viano, Eur. Phys. J. A **10**, 157 (2001).
[2] R. Fioravanti and G. A. Viano, Phys. Rev. C **55**, 2593 (1997).
[3] G. A. Viano, Phys. Rev. C **36**, 933 (1987).
[4] G. A. Viano, Phys. Rev. C **37**, 1660 (1988).
[5] V. De Alfaro and T. Regge, *Potential Scattering* (North-Holland, Amsterdam, 1965).
[6] This result, as well as the analytic continuation [Carlsonian interpolation of the *partial potentials* $V_s(R,R')$] [see Eq. (3)], requires a rather delicate and detailed mathematical analysis, which we plan to discuss in a mathematical physics journal.
[7] *Higher Trascendental Functions*, edited by A. Erdelyi (McGraw-Hill, New York, 1953), Vol. 1.
[8] A. Sommerfeld, *Partial Differential Equations in Physics* (Academic, New York, 1964).
[9] H. M. Nussenzveig, *Causality and Dispersion Relations* (Academic, New York, 1972) (in particular, see Fig. 7.3, p. 320).
[10] E. De Micheli, G. Monti Bragadin, and G. A. Viano, Rev. Math. Phys. **12**, 849 (2000).
[11] H. M. Nussenzveig, J. Math. Phys. **10**, 2 (1969); **10**, 125 (1969).
[12] S. A. Afzal, A. A. Z. Ahmad, and S. Ali, Rev. Mod. Phys. **41**, 247 (1969).
[13] B. Buck, H. Friedrich, and C. Wheatley, Nucl. Phys. **A275**, 246 (1977).
[14] W. S. Chien and R. E. Brown, Phys. Rev. C **10**, 1767 (1974).
[15] P. Darriulat, G. Igo, H. G. Pugh, and H. D. Holmgren, Phys. Rev. **137**, B315 (1965).
[16] T. A. Tombrello and L. S. Senhouse, Phys. Rev. **129**, 2252 (1963).
[17] S. Okai and S. C. Park, Phys. Rev. **145**, 787 (1966).
[18] K. Wildermuth and W. McClure, in *Springer Tracts in Modern Physics* (Springer, Berlin, 1966), Vol. 41.
[19] For a more detailed analysis of this topic and for a numerical comparison between the α-α phase shifts computed with and without the exact exchange Coulomb interaction, the interested reader is referred to Appendix B of Ref. [20] (see, in particular, Fig. 21 of this appendix).
[20] Y. C. Tang, M. LeMere, and D. R. Thompson, Phys. Rep. **47**, 167 (1978).
[21] J. Reignier, Nucl. Phys. **54**, 225 (1964).
[22] J. Reignier, Bull. Cl. Sci., Acad. R. Belg. **48**, 179 (1962).
[23] M. Bertero and G. A. Viano, Nucl. Phys. **B1**, 317 (1967).
[24] F. Ajzenberg-Selove, Nucl. Phys. **A490**, 1 (1988).
[25] R. E. Cutkosky, C. P. Forsyth, R. E. Hendrick, and R. L. Kelly, Phys. Rev. D **20**, 2839 (1979).
[26] T. P. Vrana, S. A. Dytman, and T. S. H. Lee, Phys. Rep. **328**, 181 (2000).
[27] W. F. Baker *et al.*, Nucl. Phys. **B25**, 385 (1971).
[28] A. J. Lennox *et al.*, Phys. Rev. D **11**, 1777 (1975).
[29] R. H. Dalitz, in *The Quark Model*, edited by J. J. J. Kokkedee (Benjamin, New York, 1969).
[30] We have already treated in I the generation of even and odd rotational bands starting from the dynamics of the three-body problem. We intend to present elsewhere a more detailed analysis of this type of bands in the specific case of confining potentials acting among three quarks.
[31] K. Hagiwara *et al.*, Particle Data Group, Phys. Rev. D **66**, 010001 (2002) (URL: http://pdg.lbl.gov).
[32] Beyond $E \sim 1.5$ GeV reaction and inelastic channels open, and formula (39) should be changed accordingly. However, since the sequence of resonances appears more visible in the total cross-section data than in the elastic one (see Ref. [31]), and to avoid the proliferation of fitting parameters, with a drastic approximation we fit the total cross-section with formula (39).